Enzymatic Ligation of Large Biomolecules to DNA

Rasmus Schøler Sørensen,[†,‡,⊥] Anders Hauge Okholm,[†,‡,⊥] David Schaffert,[†,‡,⊥] Anne Louise Bank Kodal,[†,§,⊥] Kurt V. Gothelf,[†,§,⊥] and Jørgen Kjems[†,‡,⊥,*]

[†]Interdisciplinary Nanoscience Center, [‡]Department of Molecular Biology, [§]Department of Chemistry, and [⊥]Centre for DNA Nanotechnology, Aarhus University, Gustav Wieds Vej 14, DK-8000 Aarhus C, Denmark

ABSTRACT The ability to synthesize, characterize, and manipulate DNA forms the foundation of a range of advanced disciplines including genomics, molecular biology, and biomolecular engineering. In particular for the latter field, DNA has proven useful as a structural or functional component in nanoscale self-assembled structures, antisense therapeutics, microarray diagnostics, and biosensors. Such applications frequently require DNA to be modified and conjugated to other macromolecules, including proteins, polymers, or fatty acids, in order to equip the system with properties required for a particular application. However, conjugation of DNA to large molecular components using classical chemistries often suffers from suboptimal yields. Here, we report the use of terminal deoxynucleotidyl transferase (TdT) for direct enzymatic ligation of native DNA to nucleotide triphosphates coupled to proteins and other large macromolecules. We demonstrate facile synthesis routes for a range of NTP-activated macromolecules and subsequent ligation to the 3′ hydroxyl group of oligodeoxynucleotides using TdT. The reaction is highly specific and proceeds rapidly and essentially to completion at micromolar concentrations. As a proof of principle, parallelly labeled oligonucleotides were used to produce nanopatterned DNA origami structures, demonstrating rapid and versatile incorporation of non-DNA components into DNA nanoarchitectures.

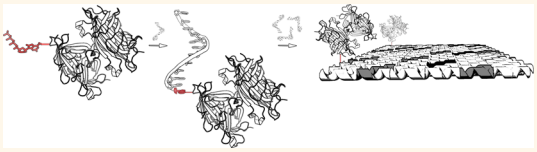

KEYWORDS: DNA nanotechnology · enzymatic ligation reaction · nucleotide triphosphate · protein–oligodeoxynucleotide conjugation · terminal deoxynucleotidyl transferase

Efficient conjugation of DNA to polymers, proteins, and other biomolecules is of particular importance in the developing field of DNA nanotechnology,[1−8] where the reliable and predictable self-assembly of DNA is used to produce well-defined nanoscale structures of arbitrary shapes.[5,6] It has proven to be a versatile platform with application in such different fields as drug delivery and therapeutics,[9,10] semiconductor–biocomplex interfaces,[11] algorithmic self-assembly,[3,12] and highly parallel computing,[3,13] and it has been applied as a research tool aiding characterization of other biological systems by NMR,[14] AFM,[15] and other techniques.[16,17] Although structurally diverse, DNA nanoscale structures lack the chemical and structural diversity found in, for example, proteins and their broader functional range of amino acids. Therefore, functional applications for DNA structures are facilitated by incorporation of peptides or other polymers to augment the properties and abilities of the system. Protein–DNA hybrid systems[4,18] are particularly interesting, allowing engineers to combine the specialized and highly optimized function of a protein with the sequence-dependent assembly of DNA, afforded by the specificity of Watson–Crick base pairing. However, the relatively low efficiency by which proteins and other polymers can be conjugated to DNA and DNA-based structures provides a challenge for production of DNA-hybrid systems. We have previously demonstrated a scheme employing the enzyme terminal deoxynucleotidyl transferase (TdT; alternatively known as DNA nucleotidylexotransferase [EC 2.7.7.31]) to extend the 3′ end of oligodeoxynucleotides with nucleotide triphosphates (NTPs) containing small chemical modifications for production of patterned DNA origami structures.[19] This scheme, however, relies on protein–ligand interactions, attaching the macromolecule noncovalently after the initial origami assembly.

Here, we present a novel, versatile, and efficient method for direct ligation of polymers, proteins, and other biomolecules to native DNA. It is based on the observation that TdT can accept nucleoside triphosphates tethered to large biomolecules as substrates and direct the ligation of the biomolecules to the 3′ end of any native oligodeoxynucleotide. The reaction proceeds rapidly and

* Address correspondence to (J. Kjems) jk@mb.au.dk.

Received for review July 3, 2013 and accepted August 8, 2013.

Published online August 08, 2013
10.1021/nn403386f

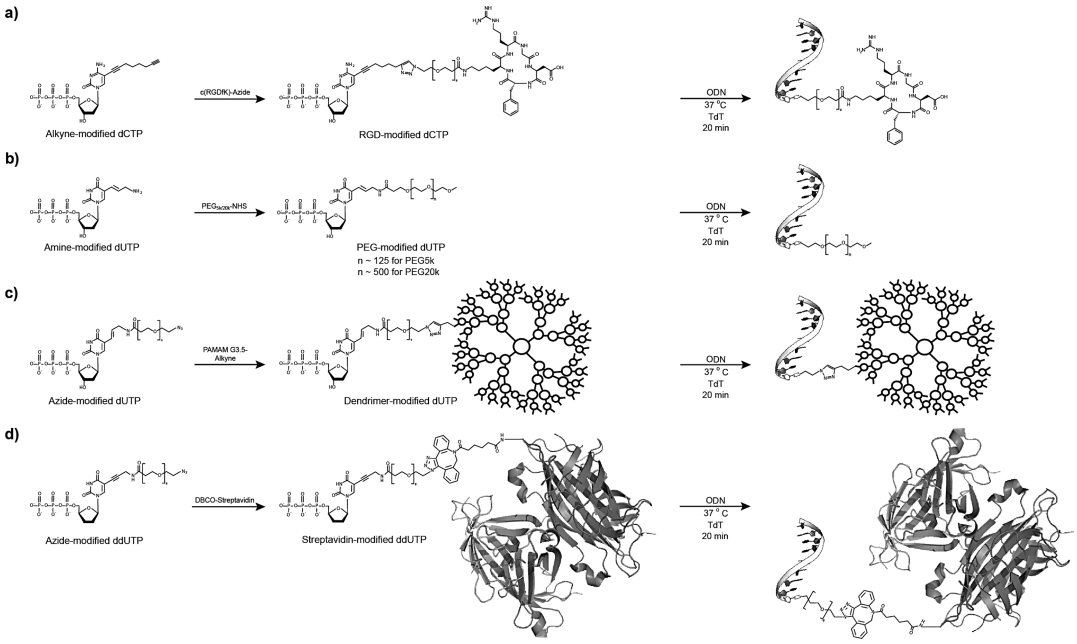

Figure 1. Synthesis routes for the four types of NTP-activated macromolecules: (a) cRGD peptide conjugation to dCTP, (b) 5 and 20 kDa PEG conjugation to dUTP, (c) G3.5 PAMAM dendrimer conjugation to dUTP, and (d) streptavidin (STV) conjugation to ddUTP. The NTP-activated macromolecules are readily applicable to enzymatic ligation to the 3′ end of an oligodeoxynucleotide, as illustrated to the right in each panel.

quantitatively under mild, aqueous conditions even using large macromolecules at micromolar concentrations, generally eliminating tedious purification of the conjugated product. TdT has previously been reported to be substrate promiscuous, particularly in the presence of cacodylate buffer and cobalt ions,[20] but previous reports have focused on NTP analogues with relatively small modifications.[21]

RESULTS AND DISCUSSION

To demonstrate the versatility of the enzymatic ligation-based method reported herein, five different macromolecules were NTP-functionalized, as outlined in Figure 1, and then enzymatically ligated to an oligodeoxynucleotide using TdT, as shown in Figure 2. The chosen macromolecules belong to different structural classes but share their common application in the fields of DNA nanotechnology and drug delivery. Cyclic integrin targeting peptide c(RGDfK)[22] was chosen as a model for peptides, while two poly(ethylene glycol) (PEG) polymers of different length served as model compounds for the introduction of high molecular weight linear polymers. A G3.5 PAMAM dendrimer, frequently used in drug delivery and ligand presentation applications, served as a model for globular polymers, and streptavidin (STV) was used as a model for introduction of proteins. Deliberately avoiding the notoriously difficult synthesis of customized NTPs, we opted for conjugation strategies compatible with commercially available NTPs. Polytriazole-catalyzed variants of the azide−alkyne cycloaddition[23] were employed for NTP activation of cRGD and the PAMAM dendrimer. In both cases high conversion was observed together with an acceptable isolated yield after purification. NTP activation of STV was completed using a copper-free DBCO-mediated click reaction,[24] and a 2-fold excess of ddUTP-DBCO was found to produce an optimal degree of STV activation. NTP activation of PEG derivatives was performed using commercially available PEG-NHS esters. Incubation of amino-modified dUTP (aa-dUTP) with a 5-fold excess of PEG-NHS for 12 h at pH 8.0 produced the PEG-coupled nucleotide products in 90% and 40% yields for 5 and 20 kDa PEG, respectively.

Enzymatic ligation reactions of the synthesized NTP-activated macromolecules to the 3′ end of an oligodeoxynucleotide proceeded to quantitative or near-quantitative conversion, as quantified by PAGE analysis of unpurified reagents, *cf.* Figure 2 and Supporting Information Figure S2. All reactions achieved a 99% conversion or better except for streptavidin, which yielded 93% STV-labeled product and 6% azido-ddUTP-capped product. Surprisingly, multiple copies of cRGD-dCTP were frequently added to the oligonucleotide template by the TdT (one, two, or three cRGD peptides added in conversions of 6%, 62%, and 32%, respectively), demonstrating that cRGD-functionalized 3′-nucleotides also can function as an acceptor in the TdT-catalyzed reaction. If a single cRGD addition is desired, a dideoxynucleotide should be used in place of dUTP. Using this strategy full conversion to the single RGD-labeled product was obtained (Supporting Figure S5). Enzymatic ligation of a G3.5 PAMAM dendrimer to the oligodeoxynucleotide resulted in a quantitative conversion (99.9%) but with a rather polydisperse ligation product. This

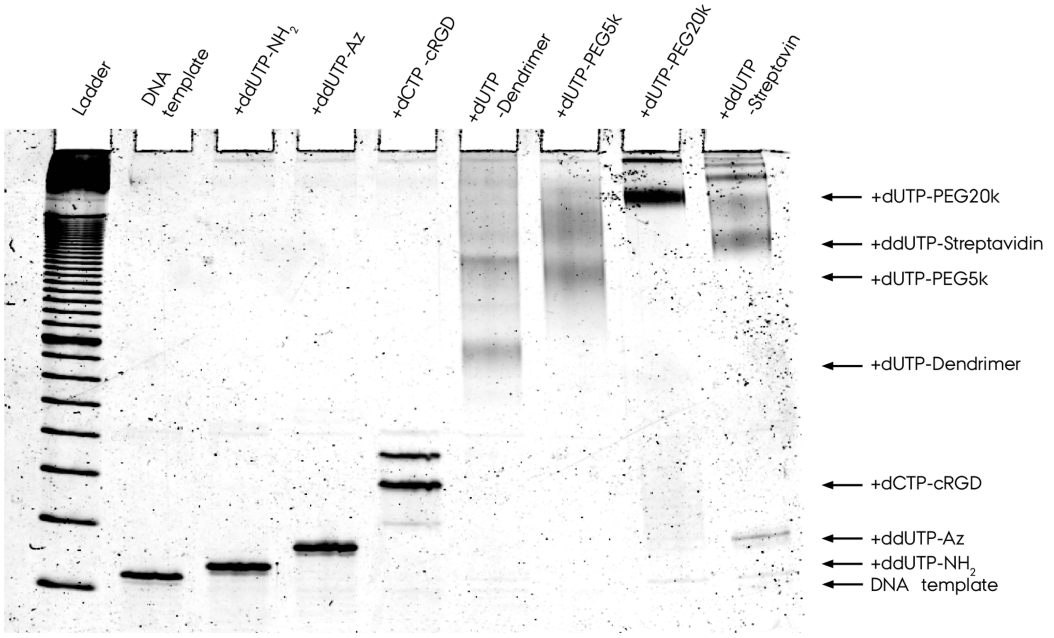

Figure 2. Gel shift mobility assay of DNA conjugated to various macromolecules *via* enzymatic ligation. Lane 1: 10 bp ladder; lane 2: DNA substrate; lanes 3−9: products of enzymatic labeling with different modified nucleotides (indicated by "+" in header). Changes in oligonucleotide mobility indicate ligation products with one or in some cases multiple NTP-activated macromolecules to the 3′ terminus of the oligonucleotide. No purification was performed after ligation reactions, clearly demonstrating the efficacy of the reaction.

correlates with the polydispersity observed by MS characterization of the dendrimer (data not shown), but may also be explained by ligation of several dendrimers to the same oligonucleotide or ligation of several oligonucleotides to polyfunctionalized dendrimers. Essentially full conversion (100% and 99.3%) was also obtained for ligation of 5 and 20 kDa PEG, respectively. The 5 kDa PEG conjugation product shows a broad size distribution, attributed to the polydispersity of the PEG chain. TdT was also capable of adding more than one 5 kDa PEG-tethered deoxynucleotide to the oligonucleotide substrate (Supporting Information Figure S1). Ligation of NTP-activated STV to the 32-mer oligodeoxynucleotide showed near-quantitative (93%) conversion, observed as four high-molecular-weight DNA−protein bands, assumed to be to mono-, di-, tri-, and tetrameric forms of STV. One faint band (6% intensity) migrates, similar to the ligation product with azido-ddUTP, indicating that a small amount of azido-ddUTP was carried over from the initial NTP activation of STV. Any dideoxynucleotide impurity present in the ligation reaction will effectively cap the oligodeoxynucleotide, rendering it inaccessible for further enzymatic conjugation. This can be mitigated by employing azido-dUTP in place of azido-ddUTP. The faint band present 2 mm into the gel in all TdT reactions is caused by the TdT reaction buffer (Supporting Information Figure S4). The results illustrate that TdT-catalyzed conjugation of large macromolecules to DNA proceeds rapidly and quantitatively using substrates markedly different from the enzyme's natural substrate.

The elimination of an intermediate purification step of conjugated products enables "one-pot" functionalization of multiple DNA strands of heterogeneous length, a feature particularly useful for DNA origami functionalization. Demonstrating the application of enzymatic ligation for rapid production of patterned DNA origami structures, we produced STV- and dendrimer-patterned tall rectangle[5] DNA origami structures. AFM imaging demonstrated successful incorporation of STV into the origami structures upon annealing with STV-coupled staple strands (Figure 3a). Reliable registration of STV on the patterned origami structures required a higher probe set-point than for previously used biotin-mediated STV binding,[19] which could indicate extra flexibility provided by the dPEG8 linker between nucleotide and STV, as well as the expected exterior coupling point on STV (Supporting Information Figure S3). Dendrimers were equally well incorporated (Figure 3b), and the use of biotin-functionalized dendrimers provided good visualization of the dendrimer locations after incubating the biotin-dendrimer-origami structures with streptavidin.

The method presented here differs significantly from previously published strategies for functionalization of DNA nanostructures. First, batchwise functionalization of multiple staple strands can be completed in a short, one-step reaction, with a conversion efficiency that frequently eliminates the need for postlabeling purification. This enables high-throughput production of a spectrum of nanopatterned structures, applicable, for example, for screening of origami-based sensors,

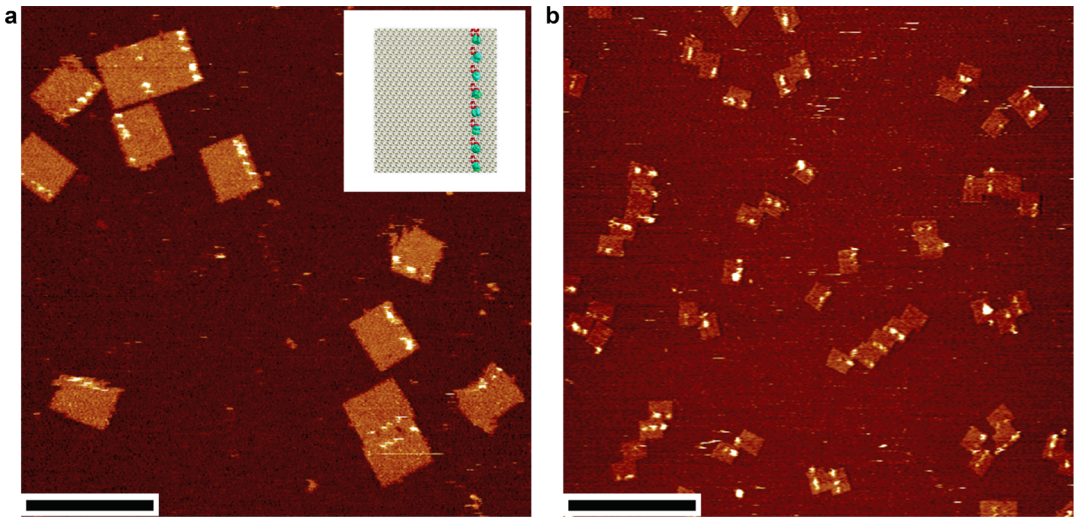

Figure 3. Application of the enzymatic labeling scheme for production of covalently patterned DNA origami. AFM images of DNA origami structures with covalently attached proteins (a) and dendrimers (b). Structures were produced *via* enzymatic ligation of NTP-activated streptavidin or G3.5 PAMAM to a selected subset of origami staple strands followed by direct annealing to the M13 scaffold together with remaining unlabeled staple strands. Inset: Origami design and expected protein locations for structures in panel a (not to scale). The designed structure in panel b is similar, but the labeled strands were offset by two columns. Scale bars: 200 nm (panel a) and 500 nm (panel b).

drug-carriers, and novel enzymatic activities. Second, the macromolecules are covalently conjugated to the staple strands of the origami structure and do not require hybridization to an external DNA handle nor is it dependent on biotin–streptavidin or other noncovalent interactions, rendering the scheme readily extendable for incorporation of enzymes and other proteins without the need for biomolecular engineering. The method has several noteworthy advantages over traditional DNA–protein conjugation schemes: The scheme can be applied directly to unmodified DNA, eliminating the need to synthesize or purchase DNA with non-natural functional groups. The enzymatic ligation proceeds rapidly and with nearly 100% conversion, thus significantly reducing the time required for reaction optimization and product purification. The reaction provides a superior level of specificity, thereby avoiding potential chemical side reactions. The scheme can be employed using commercially available nucleotides, eliminating the requirement for expert chemical skills.

In our present work we have made no attempts to conjugate the DNA to specific sites on the proteins; however we note that a majority of site-specific protein labeling methods proceeds *via* incorporation of small molecules, providing chemical handles for downstream reactions. Such site-specific labeling methods should thus be readily extendable to introduction of a ribo-triphosphate moiety, making the scheme amenable to enzymatic ligation to DNA *via* the scheme presented herein. Site-specific incorporation of triphosphates may be of particular use in protocols where orthogonal chemistries are required for multiple conjugations. The NTP-activated ligation reaction presented here shares many traits with the popular azide–alkyne "click reaction", including reliable, quantitative conversion and relatively high stability toward hydrolysis. In our hands, triphosphate-based conjugation has proven far superior to other widely used alternatives, including NHS esters, maleimides, and hydrazines, for conjugation of biomolecules to DNA. The advent of synthetic biology may make production and use of triphosphate-activated biomolecules even more interesting. Enzymes could be engineered to accept a diverse range of triphosphate-activated biomolecules for use in, for example, site-specific labeling of proteins and other substrates, thereby making triphosphate species a more broadly applicable supplement to azides as a kinetically stable high-energy functional group for aqueous bioconjugation. Since triphosphate-coupled molecules are already ubiquitous in natural systems, it might even be possible to engineer organic systems that produce ready-to-use triphosphate-activated biomolecules.

The crystal structure of terminal transferase[25] visualized in Supporting Information Figures S6 and S7 suggests why TdT is able to accept nucleotides with very large modifications on the nucleobase. The nucleobase is facing toward a wide, open crevice no more than 2 nm from the outer sphere of the enzyme. This could allow binding of the macromolecule-coupled nucleotide at the active site without significant steric interference between the enzyme and the macromolecule. Additionally, the substrate DNA strand is situated away from the open crevice in a way that would also not cause significant additional interference (Supporting Information Figure S7). The results do call for the currently accepted functional mechanism of the enzyme to be slightly amended. The existing view

assumes that the nucleotide diffuses to the active site through the central hole of the doughnut-shaped enzyme, where it is coupled to a DNA substrate situated on the opposite side of the doughnut structure.[21,25] As evident from Supporting Information Figures S6 and S7 and the accompanying Supplementary Discussion, this would not be compatible with incorporation of macromolecule-coupled nucleotides, arguing that nucleotides also can approach the active site from the face of the enzyme that binds the DNA substrate.

CONCLUSION

In conclusion, we have demonstrated efficient enzymatic ligation of DNA to macromolecules, producing DNA conjugates with polymers, proteins, and other large biomolecules using the TdT enzyme. The method enables rapid single-step conjugation of the 3′-terminal hydroxyl group in native DNA to any type of biomolecule or polymer with quantitative conversion, with no apparent limit to the size of the macromolecule. This eliminates the need for synthesizing DNA with special, non-native functional groups. Particularly for applications requiring conjugation to a large number of different oligonucleotides, enzymatic ligation to native DNA may reduce the total cost significantly. As such, we expect this technique to be useful for a number of applications in DNA nanotechnology, *e.g.*, DNA microarray diagnostics and DNA-based high-throughput screenings of therapeutics. As a proof of concept, we displayed the use of enzymatic macromolecule labeling of DNA staple strands followed by incorporation into a DNA origami structure, thereby demonstrating the versatility of the method for functionalization of DNA nanostructures.

METHODS

Materials. DNA oligodeoxynucleotides were acquired from DNA Technology (Risskov, Denmark) or IDT (Coralville, IA, USA). Unless stated otherwise, all ligations were done using a 32 nt oligodeoxynucleotide with sequence AAC CTA CCG CGA ATT ATT CAT TTC ACA TCA AG. Recombinant terminal transferase was acquired from Roche Applied Science (Indianapolis, IN, USA). Nucleotide triphosphates were acquired from Jena Bioscience (Jena, Teltow, Germany). NHS- and azide-activated PEG were acquired from IRIS Biotech GmbH (Marktredwitz, Germany). Tris(3-hydroxypropyltriazolylmethyl)amine (THTA) ligand was synthesized as previously published.[26] G3.5 carboxylate PAMAM dendrimers (ethylene diamine core) were purchased from Sigma-Aldrich (10% in methanol) and alkyne-functionalized using a previously published procedure.[27] Azido-dPEG8-NHS and DBCO-NHS were obtained from Quanta Biodesign. Cyclic RGD peptide, c(RGDfK), was acquired from Anaspec, while Cyclo(RGDfK)-PEG-azide (used for Supporting Figure S5) was purchased from Peptides International Inc. (Louisville, KY, USA). Streptavidin from *Streptomyces avidinii* was acquired from Sigma-Aldrich and SYBR Gold from Invitrogen. Unless specified otherwise, all water was type 1 grade produced by a Milli-Q water purification system (or equivalent), and all solvents were p.a. grade.

Nucleotide Synthesis. Nucleotide triphosphate derivatives were synthesized as follows: ddUTP-5-propargylamino-dPEG8-N_3 (ap-ddUTP) was synthesized by mixing 150 nmol of 5-propargylamino-2′,3′-dideoxy-uridine-5′-triphosphate (ddUTP) in 80 μL of HEPES buffer (50 mM, pH 7.8) with 600 nmol of azido-dPEG8-NHS in 6 μL of DMSO, followed by stirring for 16 h at RT. The crude product was purified by RP-HPLC on an analytical Phenomenex Kinetex XB-C18 column (150 × 4.6 mm) using a TEAA/MeCN gradient buffer system (buffer A: 50 mM TEAA pH 7.0; buffer B: MeCN; 5% B to 40% in 20 min, 1 mL/min). The product-containing fractions were pooled, freeze-dried, and dissolved in water to a concentration of 5 mM, confirmed by UV absorption at 289 nm. Isolated yield was 100 nmol (66%). ddUTP-DBCO was synthesized by reacting 0.5 μmol of ddUTP in 200 μL of HEPES buffer (50 mM, pH 7.8) with 2.5 μmol of DBCO-NHS in 250 μL of DMSO under stirring for 16 h at RT. The crude product was purified by RP-HPLC on an analytical Phenomenex Kinetex XB-C18 column (150 × 4.6 mm) using a TEAA/MeCN gradient buffer system (buffer A: 50 mM TEAA pH 7.0; buffer B: MeCN; 5% B to 80% in 24 min, 1 mL/min). The product-containing fractions were pooled, freeze-dried, and dissolved in water to a concentration of 5 mM, confirmed by UV absorption at 310 nm ($\varepsilon = 13.45 \times 10^3$ cm^{-1} M^{-1}). Isolated yield was 250 nmol (50%). To synthesize ddUTP-5-propargylamino-pentyne, 5-propargylamino-2′,3′-dideoxy-uridine-5′-triphosphate (1 equiv, 150 nmol) in 80 μL of HEPES buffer (50 mM, pH 7.8) was mixed with a solution of pentynoic-NHS (4 equiv, 600 nmol, 6 μL) in DMSO p.a. and stirred for 16 h at RT. The crude product was purified by RP-HPLC on an analytical Phenomenex Kinetex XB-C18 column (150 × 4.6 mm) using a TEAA/MeCN gradient buffer system (buffer A: 50 mM TEAA pH 7.0; buffer B: MeCN; 5% B to 40% in 20 min, 1 mL/min). The product-containing fractions were pooled and freeze-dried. The freeze-dried nucleotide was dissolved in nuclease-free water to a concentration of 5 mM (confirmed by UV absorption at 289 nm). Isolated yield was 75%. To synthesize azido-functionalized cRGD peptide, 500 nmol of c(RGDfK) in 90 μL of HEPES buffer (100 mM, pH 8.0) was mixed with 2.5 μmol of azido-dPEG8-NHS in 25 μL of DMSO and stirred for 16 h at RT. The crude product was purified by RP-HPLC on an analytical Phenomenex C18 column (250 × 4.6 mm) using a TFA/MeCN gradient buffer system (buffer A: 0.1% TFA pH 2.5; buffer B: MeCN; 5% B to 40% in 33 min, 1 mL/min). The product-containing fractions were pooled, freeze-dried, and dissolved in water to a concentration of approximately 5 mM, confirmed by UV absorption at 255 nm (phenylalanine) using a cRGD standard curve. Isolated yield was 225 nmol (45%). NTP activation was performed by reaction of 100 nmol of c(RGDfK)-dPEG8-N3 with 50 nmol of 5-(octa-1,7-diynyl)-2′-deoxycytidine 5′-triphosphate (alkyne-C8-dCTP) in a final volume of 75 μL of HEPES buffer (10 mM, pH 7.8). The reaction was initiated by addition of $CuSO_4$ (472 μM), THTA (2.8 mM), and sodium L-ascorbate (18.3 mM) and shaken at 450 rpm for 3 h at 37 °C. The product was purified on reversed-phase HPLC, freeze-dried, and redissolved in 40 μL of water. A dideoxynucleotide-activated cRGD (for Supporting Figure S5) was synthesized by reaction of 100 nmol of c(RGDfK)-PEG-PEG-N3 with 50 nmol of ddUTP-5-propargylaminopentyne in a final volume of 90 μL of DMSO/HEPES-buffer (1:1, 20 mM, pH 7.8). The reaction was initiated by addition of $CuSO_4$ (445 μM), TBTA (890 μM), and sodium L-ascorbate (16.7 mM) and shaken at 450 rpm for 16 h at 24 °C. The product was purified on reversed-phase HPLC (analytical Phenomenex Kinetex XB-C18 column, 150 × 4.6 mm) using a TEAA/MeCN gradient buffer system (buffer A: 50 mM TEAA pH 7.0; buffer B: MeCN; 5% B to 40% in 20 min, 1 mL/min). The product-containing fractions were pooled, freeze-dried, and redissolved in 50 μL of water. Isolated yield was 80%. NTP-activated dendrimers were synthesized by mixing 40 nmol of azido-PEG4-aminoallyl-dUTP (5-(15-azido-4,7,10,13-tetraoxa-pentadecanoyl-aminoallyl)-2′-deoxy-uridine-5′-triphosphate, apa-dUTP) with 200 nmol of G3.5 alkyne dendrimer and DMSO (12% v/v), $CuSO_4$ (200 μM), THTA (1.6 mM), HEPES buffer (100 mM, pH 7.5), and sodium L-ascorbate (20 mM) to a final volume of 1 mL. The mixture was reacted for 75 min, and excess reagents were removed using a

3 kDa MWCO Amicon Ultra spin-dialysis filter and washed three times with water. The retentate was recovered, and UV-spectrum analysis displayed characteristic dendrimer and NTP absorbance patterns. PEG of size 5 and 20 kDa was NTP-activated by reacting 300 nmol of PEG-NHS with 50 nmol of 5-(3-aminoallyl)-2′-deoxy-uridine-5′-triphosphate (aa-dUTP) in 100 μL of HEPES buffer (80 mM, pH 8). The reactions were shaken at 500 rpm overnight. PEG5k-aa-dUTP was used without further purification (>95% conversion), while the reaction with 20 kDa PEG was shown to be incomplete (Supporting Information Figure S1). Thus, the 20 kDa PEG-dUTP product was purified using 10 kDa MWCO Amicon Ultra spin-dialysis filters (14000*g*, 30 min, 4 °C) and washed twice with water. Alternatively, for applications requiring a pure product, the crude product was purified by RP-HPLC on an analytical Phenomenex Kinetex XB-C18 column as described above. For NTP activation of streptavidin a copper-free click reaction was employed, as initial activation studies using TBTA catalysis led to severe precipitation problems. It was found that the DBCO-mediated reaction provided reliable modification of biomolecules without the additional complication of optimizing a multicomponent conjugation reaction. NTP activation of streptavidin used for Figure 2 was done as follows: 24 nmol of STV and 600 nmol of DBCO-NHS (dibenzylcyclooctyne-*N*-hydroxysuccinimide ester, 100 mM in DMSO) were mixed in 480 μL of HEPES buffer (37.5 mM, pH 8.0) and DMSO (25% v/v) and left to react for 2 h at RT. The product was diluted 10-fold and purified using 10 kDa MWCO Amicon Ultra spin-dialysis (10000*g*, 20 min, 4 °C) and washed three times with water. A 25 μL amount of recovered product was diluted 1:1 with water, and 30 μL was subsequently reacted with 7.5 nmol of ap-ddUTP in 55 μL of HEPES buffer (36 mM, pH 7.8) for 16 h at RT. STV-ddUTP was purified using 10 kDa MWCO Amicon Ultra spin-dialysis filters as above, but washed with NaCl (250 mM) twice and finally in water. It was found that no mixture of DMSO and aqueous buffer could retain both STV and DBCO-NHS in solution. Thus, the scheme for synthesizing STV-ddUTP used for Figure 3 was adjusted slightly: 4.4 nmol of STV and 50 nmol of NHS-dPEG8-N3 were mixed with DMSO (12.5% v/v) and HEPES-KCl-buffer (12.5 mM, pH 8.0) in a total volume of 40 μL and shaken at 900 rpm for 2 h at RT. Then 400 μL of HEPES buffer (10 mM, pH 8.0) with KCl (50 mM) was added to reduce DMSO concentration followed by purification on 3 kDa MWCO Amicon Ultra spin-dialysis (14000*g* for 10 min) and washed five times with the same buffer; 68% STV was recovered, confirmed by UV absorption at 280 nm. The 50 μL of collected retentate was mixed with 8 nmol of DBCO-ddUTP and incubated at 5 °C overnight, then shaken at 950 rpm for 1 h at RT. Unreacted DBCO-ddUTP was removed by diafiltration using 10 kDa MWCO Amicon Ultra spin-dialysis filters (14000*g* for 10 min) and washed three times.

Enzymatic Ligation of NTP-Activated Biomolecules to DNA. Unless stated otherwise, ligation reactions consisted of the following components: DNA (2 μM), NTP-activated biomolecules (20 μM) with terminal transferase enzyme (20 U/μL), cacodylate (0.2 M) and Tris-HCl buffer (0.125 M, pH 6.6), $CoCl_2$ (5 mM), and BSA (0.25 mg/mL). The reaction mixture further included 5% enzyme storage buffer consisting of K_2HPO_4 (60 mM, pH 7.2), KCl (150 mM), 2-mercaptoethanol (1 mM), Triton X-100 (0.5%), and glycerol (50%). Ligation reactions were performed in a total reaction volume of 8 μL and left at 37 °C for 20 min (25 min for dendrimers). Reactions were terminated by addition of EDTA (20 mM, pH 8.0). DNA−biomolecule conjugation products were analyzed by denaturing polyacrylamide gel electrophoresis. Gels were typically cast as 10% polyacrylamide with 7 M urea, prerun for 30 min, and run with samples for 1 h in 1× TBE running-buffer at 20 W (500 V, 17 cm in length). Gels were stained with SYBR Gold and visualized on a GE Healthcare Typhoon Trio gel scanning system with recommended filter settings. GE Healthcare ImageQuant software was used for image processing and band quantification.

Origami Annealing and AFM. Tall rectangle[5] origami structures were designed to have the nicks of the labeled staple strands positioned on the opposite side relative to the original structure. This side has previously been shown to be the side predominantly facing upward after adsorbing the origami to a mica substrate.[5,19] Staple strands for the DNA origami structure were pooled from the plates using custom-written software and a pipetting robot. Selected staple strands were efficiently ligated to STV after 1.5 h, as confirmed by PAGE analysis. STV-patterned origami was annealed using an M13mp18 scaffold (4 nM) and staple strands (40 nM) with $Mg(OAc)_2$ (10 mM) and 1× TAE buffer using a 12 h thermal gradient going from 80 °C to 15 °C. Dendrimer-modified staple strands were functionalized with a biotin-azide prior to origami assembly by mixing biotin-azide (120 μM), alkyne-dendrimer-dUTP (2 μM), $CuSO_4$ (0.2 mM), THTA-ligand (1.6 mM), sodium L-ascorbate (20 mM), HEPES (100 mM, pH 7.5), and DMSO (12%) and incubating at RT for 30 min followed by purification *via* diafiltration with 3K MWCO Amicon filters as previously described. Dendrimer-patterned origami was annealed under conditions similar to STV-labeled origami, but using a 10 nM scaffold and 60 nM staples, followed by postassembly agarose purification to remove excess dendrimers. Streptavidin was added during AFM imaging of biotin-dendrimer-labeled origami structures to augment visualization of the otherwise unstructured dendrimers. Liquid tapping mode AFM imaging was done on an Agilent 5500 AFM using a Bruker silicon nitride probe model OTR4-10 with a spring constant of 0.02 N/m with parameters as previously described.[19] Image processing was done with Scanning Probe Image Processing software from Image Metrology.

Conflict of Interest: The authors declare no competing financial interest.

Supporting Information Available: PAGE and AFM data, structural representations of TdT, and supporting discussion on the structural basis of substrate promiscuity of TdT. This material is available free of charge *via* the Internet at http://pubs.acs.org.

Acknowledgment. R.S.S., A.H.O., D.H.S., and A.L.B.K. synthesized intermediary and final nucleotides. R.S.S. and A.H.O. performed PAGE analysis of ligation products. R.S.S. and A.L.B.K. performed AFM imaging of streptavidin- and dendrimer-modified origami. R.S.S. conceived the project, and J.K. and K.V.G. supervised the project. R.S.S., A.H.O., D.S., and J.K. produced the manuscript. The authors would like to thank the Danish National Research Foundation for funding (Grant No. DNRF78). D.S. was supported by Villum Kann Rasmussen Foundation and BioNEC, a centre of Excellence funded by The Villum Foundation for studies on biomolecular nanoscale engineering. R.S.S. would like to thank M. Kwak at the Wyss Institute of Biologically Inspired Engineering at Harvard University, Boston, for input on the structural basis for substrate promiscuity of TdT.

REFERENCES AND NOTES

1. Chen, J.; Seeman, N. C. Synthesis from DNA of a Molecule with the Connectivity of a Cube. *Nature* **1991**, *350*, 631–633.
2. Winfree, E.; Liu, F.; Wenzler, L. A.; Seeman, N. C. Design and Self-Assembly of Two-Dimensional DNA Crystals. *Nature* **1998**, *394*, 539–544.
3. Mao, C.; LaBean, T. H.; Reif, J. H.; Seeman, N. C. Logical Computation Using Algorithmic Self-Assembly of DNA Triple-Crossover Molecules. *Nature* **2000**, *407*, 493–496.
4. Yan, H.; Park, S. H.; Finkelstein, G.; Reif, J. H.; LaBean, T. H. DNA-Templated Self-Assembly of Protein Arrays and Highly Conductive Nanowires. *Science* **2003**, *301*, 1882–1884.
5. Rothemund, P. W. K. Folding DNA to Create Nanoscale Shapes and Patterns. *Nature* **2006**, *440*, 297–302.
6. Douglas, S. M.; Dietz, H.; Liedl, T.; Hogberg, B.; Graf, F.; Shih, W. M. Self-Assembly of DNA into Nanoscale Three-Dimensional Shapes. *Nature* **2009**, *459*, 414–418.
7. Andersen, E. S.; Dong, M.; Nielsen, M. M.; Jahn, K.; Subramani, R.; Mamdouh, W.; Golas, M. M.; Sander, B.; Stark, H.; Oliveira, C. L. P.; *et al.* Self-Assembly of a Nanoscale DNA Box with a Controllable Lid. *Nature* **2009**, *459*, 73–76.
8. Wei, B.; Dai, M.; Yin, P. Complex Shapes Self-Assembled from Single-Stranded DNA Tiles. *Nature* **2012**, *485*, 623–626.
9. Douglas, S. M.; Bachelet, I.; Church, G. M. A Logic-Gated Nanorobot for Targeted Transport of Molecular Payloads. *Science* **2012**, *335*, 831–834.

10. Zhao, Y.-X.; Shaw, A.; Zeng, X.; Benson, E.; Nyström, A. M.; Högberg, B. DNA Origami Delivery System for Cancer Therapy with Tunable Release Properties. *ACS Nano* **2012**, *6*, 8684–8691.
11. Woo, S.; Rothemund, P. W. K. Programmable Molecular Recognition Based on the Geometry of DNA Nanostructures. *Nat. Chem.* **2011**, *3*, 620–627.
12. Rothemund, P. W. K.; Papadakis, N.; Winfree, E. Algorithmic Self-Assembly of DNA Sierpinski Triangles. *PLoS Biol.* **2004**, *2*, 2041–2053.
13. Qian, L.; Winfree, E.; Bruck, J. Neural Network Computation with DNA Strand Displacement Cascades. *Nature* **2011**, *475*, 368–372.
14. Bellot, G.; McClintock, M. A.; Chou, J. J.; Shih, W. M. DNA Nanotubes for NMR Structure Determination of Membrane Proteins. *Nat. Protoc.* **2013**, *8*, 755–770.
15. Endo, M.; Tatsumi, K.; Terushima, K.; Katsuda, Y.; Hidaka, K.; Harada, Y.; Sugiyama, H. Direct Visualization of the Movement of a Single T7 RNA Polymerase and Transcription on a DNA Nanostructure. *Angew. Chem., Int. Ed.* **2012**, *51*, 8778–8782.
16. Steinhauer, C.; Jungmann, R.; Sobey, T. L.; Simmel, F. C.; Tinnefeld, P. DNA Origami as a Nanoscopic Ruler for Super-Resolution Microscopy. *Angew. Chem., Int. Ed.* **2009**, *48*, 8870–8873.
17. Kuzyk, A.; Schreiber, R.; Fan, Z.; Pardatscher, G.; Roller, E.-M.; Högele, A.; Simmel, F. C.; Govorov, A. O.; Liedl, T. DNA-Based Self-Assembly of Chiral Plasmonic Nanostructures with Tailored Optical Response. *Nature* **2012**, *483*, 311–314.
18. Saccà, B.; Meyer, R.; Erkelenz, M.; Kiko, K.; Arndt, A.; Schroeder, H.; Rabe, K. S.; Niemeyer, C. M. Orthogonal Protein Decoration of DNA Origami. *Angew. Chem., Int. Ed.* **2010**, *49*, 9378–9383.
19. Jahn, K.; Tørring, T.; Voigt, N. V.; Sørensen, R. S.; Bank Kodal, A. L.; Andersen, E. S.; Gothelf, K. V.; Kjems, J. Functional Patterning of DNA Origami by Parallel Enzymatic Modification. *Bioconjugate Chem.* **2011**, *22*, 819–823.
20. Hatahet, Z.; Purmal, A. A.; Wallace, S. S. A Novel Method for Site Specific Introduction of Single Model Oxidative DNA Lesions into Oligodeoxyribonucleotides. *Nucleic Acids Res.* **1993**, *21*, 1563–1568.
21. Motea, E. A.; Berdis, A. J. Terminal Deoxynucleotidyl Transferase: The Story of a Misguided DNA Polymerase. *Biochim. Biophys. Acta, Proteins Proteomics* **2010**, *1804*, 1151–1166.
22. Haubner, R.; Gratias, R.; Diefenbach, B.; Goodman, S. L.; Jonczyk, A.; Kessler, H. Structural and Functional Aspects of RGD-Containing Cyclic Pentapeptides as Highly Potent and Selective Integrin $\alpha V\beta 3$ Antagonists. *J. Am. Chem. Soc.* **1996**, *118*, 7461–7472.
23. Chan, T. R.; Hilgraf, R.; Sharpless, K. B.; Fokin, V. V. Polytriazoles as Copper(I)-Stabilizing Ligands in Catalysis. *Org. Lett.* **2004**, *6*, 2853–2855.
24. Debets, M. F.; Berkel, S. S.; van Schoffelen, S.; Rutjes, F. P. J. T.; van Hest, J. C. M.; van Delft, F. L. Aza-Dibenzocyclooctynes for Fast and Efficient Enzyme PEGylation *via* Copper-Free (3+2) Cycloaddition. *Chem. Commun.* **2010**, *46*, 97–99.
25. Delarue, M.; Boulé, J. B.; Lescar, J.; Expert-Bezançon, N.; Jourdan, N.; Sukumar, N.; Rougeon, F.; Papanicolaou, C. Crystal Structures of a Template-Independent DNA Polymerase: Murine Terminal Deoxynucleotidyltransferase. *Embo J.* **2002**, *21*, 427–439.
26. Voigt, N. V.; Tørring, T.; Rotaru, A.; Jacobsen, M. F.; Ravnsbaek, J. B.; Subramani, R.; Mamdouh, W.; Kjems, J.; Mokhir, A.; Besenbacher, F.; *et al.* Single-Molecule Chemical Reactions on DNA Origami. *Nat. Nanotechnol.* **2010**, *5*, 200–203.
27. Liu, H.; Tørring, T.; Dong, M.; Rosen, C. B.; Besenbacher, F.; Gothelf, K. V. DNA-Templated Covalent Coupling of G4 PAMAM Dendrimers. *J. Am. Chem. Soc.* **2010**, *132*, 18054–18056.